Egyptian Geophysical Society
EGS Journal, Vol. 13, No. 1, 103-113 (2015)

EARTHQUAKE OF THE 27TH OF OCTOBER 2013 OF KALABSHA, ASWAN AREA, SOUTHERN EGYPT

K. Omar and G.E.A. Mohamed

Seismology Department (E-mail: khaled.yosif@yahoo.com)
National Research Institute of Astronomy and Geophysics (NRIAG)
11421- Helwan, Cairo, Egypt.

زلزال يوم ٢٧ اكتوبر ٢٠١٣ بكلابشة، منطقة أسوان، جنوب مصر

الخلاصة: في يوم الاحد ٢٧ اكتوبر ٢٠١٣ الساعة ١٣:٢١:١٥ بتوقيت جرينتش حدث زلزال بقوة ٣,٩ غرب بحيرة ناصر بأسوان ثم أعقبه زلزال آخر يوم ٢٨ اكتوبر ٢٠١٣ بقوة ٢,٧ بنفس المكان. تم تقدير آلية البؤرة للزلزالين ووجد أنها فالق زحفى مع وجود حركة عادية على سطح الفالق. وكانت إتجاهات مستويى الفالق للزلزال الأول والثانى شمال– جنوب، وشرق– غرب. تم حساب معاملات المصدر للزلزالين فكانت اللحظة الزلزالية للأول 6.18E+20 dyne.cmوللثانى 1.95E+19 dyne.cm. وانخفاض الاجهاد 0.0008 and 0.003 MPa ونصف قطر المصدر 99.79 and 98.73 m الطاقة الزلزالية الصادرة 9.74E+14 and 3.09E+16

ABSTRACT: *On Sunday October 27, 2013 at 13:21:15 (GMT) an earthquake of ML 3.9 occurred west Lake Nasser, Aswan and followed with an earthquake on Monday October 28, 2013 at 08:39:19 (GMT) with ML 2.7. Both are located at Aswan area. Moment tensor inversions of the two events reveal strike-slip mechanism with considerable normal faulting component. Derived focal mechanism of the first and of the second using polarities of P wave shows strike-slip fault with minor movement of normal type. The solutions gave two nodal planes trending N–S, E-W in close agreement with the surface traces of the faults crossing the area. The movement is right lateral along the first plane while left lateral along the second one. The source parameters were estimated and seismic moment was found to be 6.18E+20 dyne.cm for the first and 1.95E+19 dyne.cm for the second event. This corresponds to a moment magnitude Mw 3.1 and 2.1 respectively. Following Brune model, the source radius is 98.73 and 99.79 m, stress drop was 0.003 and 0.0008 MPa and seismic energy released is 3.09E+16 for first event and 9.74E+14 for the second event. The source mechanism from the fault plane solution shows a normal fault with considerable strike-slip component.*

1. INTRODUCTION

The Aswan area is located in the southern part of Egypt, between latitudes 23.00–24.00° N and longitudes 32.12–33.10° E. Such region is characterized by its strategic importance, especially after the establishment of the High Dam in 1960. The area has been subjected to numerous geological and geophysical investigations such as the structural settings and geomorphologic conditions of the study area (e.g., El-Shazly 1977 and Issawi 1978); gravity and geodesy (Mahmoud 1994); 3D Vp, Vs, and Vp/vs tomography (Taha 1997; El-Hady et al. 2004; Khalil et al. 2004); subsurface tectonic structure and crustal deformation (Mekkawi et al. 2008), and focal mechanisms of source zones (Kebeasy et al. 1987; Kebeasy and Tealeb 1997; Hassib 1997; Tealeb 1999; Fat-Helbary and Tealeb 2000; Awad et al. 2005). On Sunday October 27, 2013 at 13:21:15 (GMT) an earthquake of ML 3.9 has occurred west Lake Nasser and followed by an second event On Monday October 28, 2013 at 08:39:19 (GMT) with ML 2.7 on Kalabsha fault at Aswan area on the western bank of Lake Nasser. In this paper we estimate the inversion moment tensor and calculate the source parameters for these events.

2. TECTONIC SETTING AND SEISMICITY OF THE AREA

The major geomorphologic features of the study area from east to west are Aswan hills, the River Nile valley, Nubian plain, and Sin El-Kaddab plateau, respectively (Woodward Clyde Consultants 1985). Precambrian basement rocks are distributed in the area at small localities along the western bank of the Nile between the Kalabsha fault in the south and the city of Aswan in the north, overlain by a series of sedimentary units of Late Cretaceous–Lower Eocene, (Issawi 1978, 1982 and Woodward Clyde Consultants 1985). Figure 1 shows the general distribution of rock units and basic structural and topographic characteristics of these features.

The study area is highly affected by tectonic movements, which had a profound effect on the geomorphology of the area, leading to many uplifts, faulted blocks, and folds. Faults in the study area are subdivided into two fault systems, East–west and North–south, as shown in Fig. 2. The east–west fault system (Kalabsha, Seiyal, and Rawraw fault), which passes through the Sin El-Kaddab limestone plateau, is considered as the most active fault system in the study area.

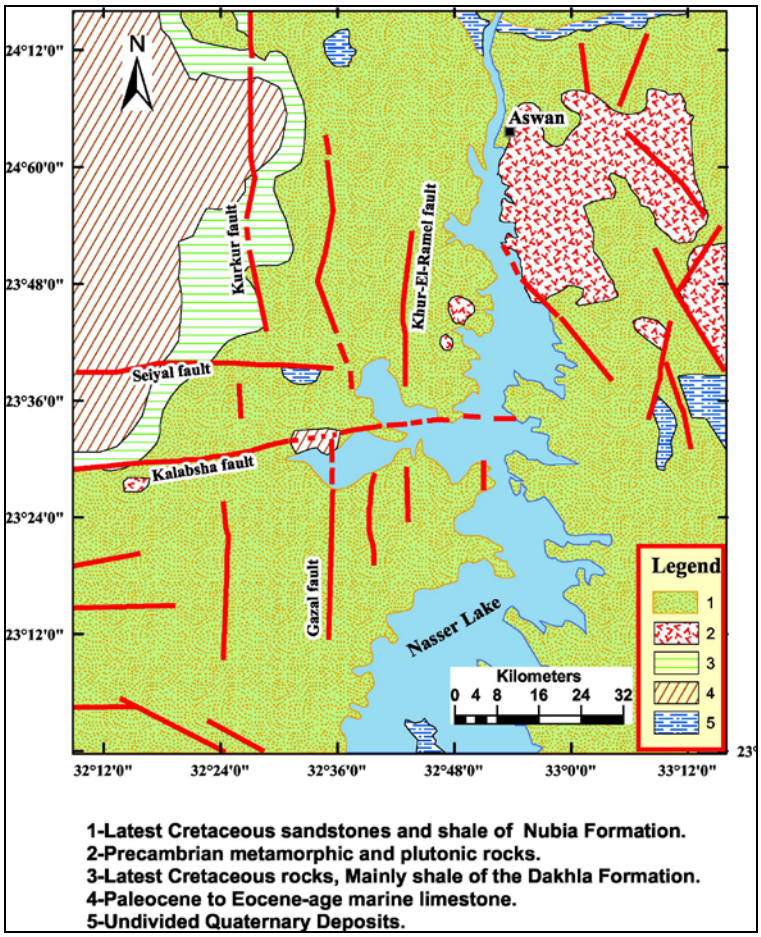

Fig. (1): Geological map of the study area.

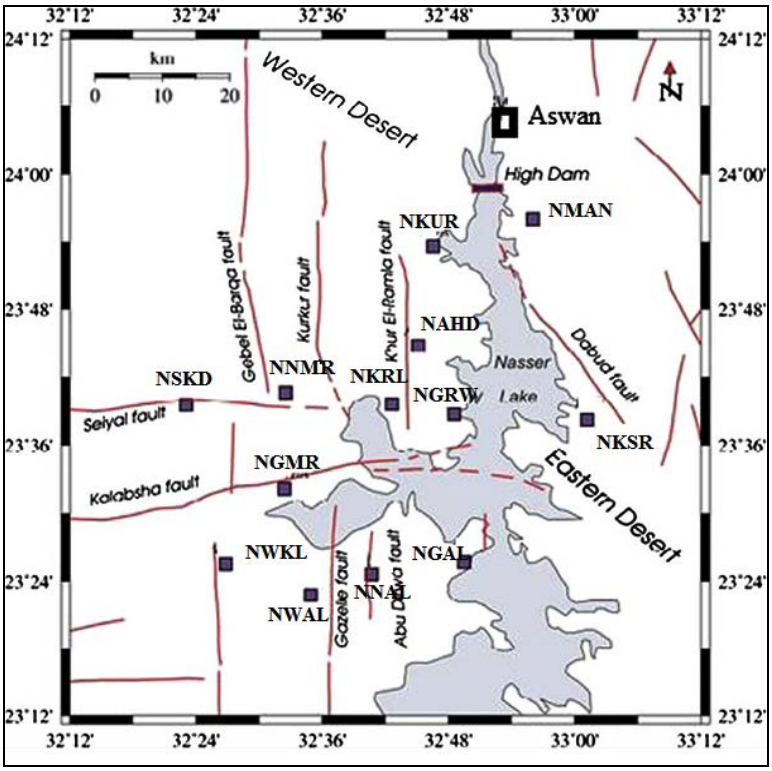

Fig. (2): Distribution of the Aswan seismic network. Squares represent seismic stations annotated by their station codes. The lines denote surface faults crossing the area (dotted where concealed).

The Kalabsha fault is trending right lateral-slip fault that is considered to have been the source of the 14 November 1981 earthquake (Kebeasy et al. 1982; Simpson et al. 1990; Awad 1994). The north–south fault systems (Kurkur, Khour El-Ramla, Gazal, and Abu-Dirwa) affectmainly the Nubian plain and are essentially of strike-slip with a normal component. Figure 2 show all faults cut the study area. The east–west and north– south fault systems affect the sandstone beds of the Nubian Plain by normal and strike-slip faults.

In 1982, after the 14 November 1981 earthquake, the National Research Institute of Astronomy and Geophysics deployed about eight analog seismic telemetric stations around the northern part of Lake Nasser. In 1985, the network was expanded to 13 telemetric stations, installed to continuously monitor the seismic activity around the northern part of Lake Nasser.

Recently, (from 2008 to 2010) with aim of expanding the frequency bands of recording, these seismic stations have modified and became broad band, and very broad band seismic stations (Fig. 2). On the other hand, a specific strong-motion network is distributed at different levels of the High Dam in order to record any trigger due to seismic activities around the Dam, especially the large events. On 14 November 1981, an earthquake of magnitude (mb = 5.5) occurred at the south of Aswan City and as a result, several studies were carried out to investigate the earthquake time and spatial distributions to determine the active seismic patterns (e.g., Woodward Clyde Consultants (WCC), 1985; Kebeasy et al. 1982; Kebeasy and Gharib 1991; Awad and Mizoue 1995; Awad 2002; Hassib 1990; Mekkawi et al. 2004). The occurrence of this event was initially thought as possibly being triggered by the presence of the reservoir (Kebeasy et al. 1987). WCC (1985) concluded that the reservoir itself does not produce earthquakes, but it serves to trigger the release of preexisting stress stored in the earth's crust. Both water load and pore pressure effects played a big role in triggering the shallower activity (Abou Elenean 2007; WCC 1985).

Figure (3) shows the seismicity map of Aswan for a period from 1997 to 2013.

3. MOMENT TENSOR INVERSION

Eight ENSN broadband (BB) seismic stations (NGAL, NGMR, NNMR, NWKL, NWAL, NMAN , NKUR and NSKD) were used for first event and (NNAl, NGMR, NNMR, NWKL, NWAL, NMAN, NKUR and NSKD for second event) were used to estimate the moment tensor for this two earthquakes (Fig. 4&5). The computer code ISOLA is used, combining the computational speed of Fortran and the users' comfort of Matlab (Sokos and Zahradnı´k 2008). It makes use of the inverse-problem formulation of Kikuchi and Kanamori (1991), based on six elementary MTs. The Green's functions are calculated by the discrete-wavenumber method (Coutant 1990; Bouchon 2003). The velocity model used to generate the Green's functions is listed in table (1).

The waveforms of the eight seismic stations are converted from the SAC format to ISOLA native format for retrieving the moment tensors. The conversion is accomplished using Matlab codes (m-files) (Thorne 2005). The waveform data pre-processing part (instrument correction, alignment, integration, decimation, etc.) is carried out carefully. These tasks are of major importance since in many cases the data contain various spurious signals, e.g., trends that can affect the inversion, while at the same time these are not easily recognizable in the time series data (Zahradnik and Plesinger 2005). The waveform correlation fit among the observed and synthetic waveforms for all used seismic stations is shown in (Fig. 4&5).

Before the final inversion result, the moment tensor calculation of this paper includes two steps. In step 1, we fix the horizontal source position (the ENSN epicenter) and repeat the waveform inversion for a set of trial depths. The correlation between observed and synthetic seismograms, as a function of depth, is shown in (Fig.6&7), illustrating the stability of the focal mechanism and the best-fitting depth of 6 km. In step 2, we seek the centroid in three horizontal planes at the depth of 4, 8, 10 and 12 km for the first event and best fitting depth of 7 km and the centroid in three horizontal planes at the depth of 12, 17 km for second event, using a 22-point grid stencils for first event and 48-point grid stencils for second event, steps of 2×2 km, all centered below the epicenter. The grid search provides a weakly varying focal mechanism and an improved centroid position at the depth of 7 km.

The inversion is done in a lower frequency band between 0.03 and 0.05 Hz. The result with the highest variance reduction for stations was selected as the final result.

In general, the full moment tensor has a deviatoric and volumetric part. Retrieval of the volumetric part is very difficult, although not impossible (e.g., Frohlich 1994; Campus and Faeh 1997; Dreger and Woods 2002). Fortunately, the inverse problem remains linear even if limited to the deviatoric moment tensor. In this study, the inversion is performed only for deviatoric moment tensor with constraint on the isotropic component, since this area is characterized by tectonic earthquakes. The deviatoric tensor can be decomposed into the double-couple (DC) and non-double-couple (non-DC) component.

Here, from a study of the Kalabsha event, based on the waveform inversion, the obtained focal mechanism is a very stable solution and indicates a strike-slip fault with minor movement of normal fault trending N–S, E-W that is consistent with major fault trends or the dominant surface faults crossing the kalabsha area, as shown in Figs. (8&9). Furthermore, this mechanism is in agreement with our obtained results implied good agreement with those previous studies.

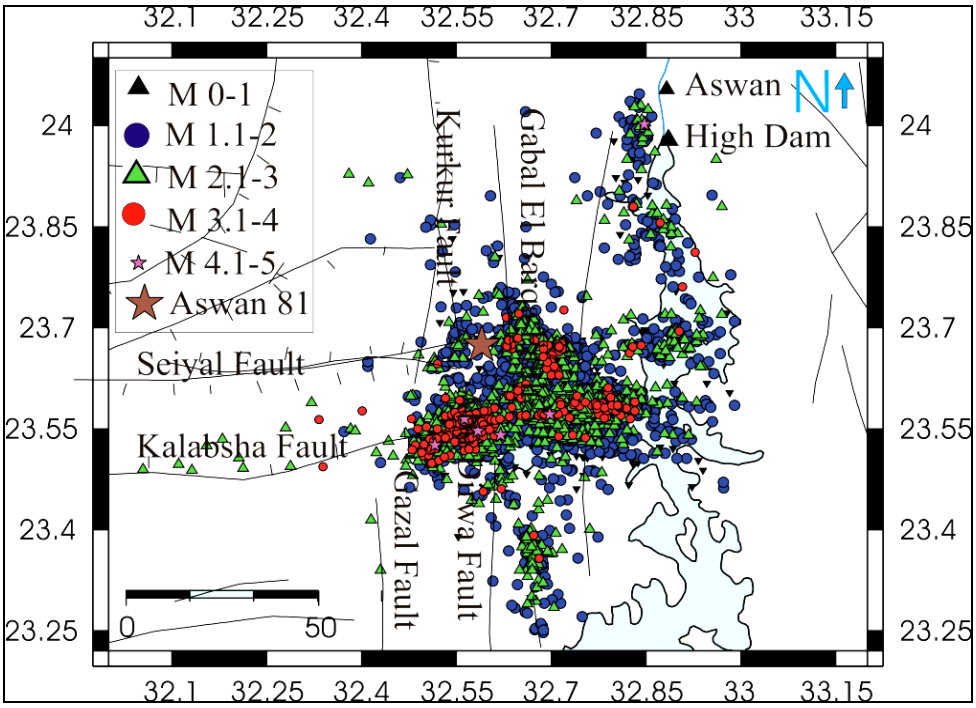

Fig. (3): Seismicity map of Aswan for a period from 1997 to 2013 (different symbols for different magnitudes). The active faults cut the study area are represented by solid lines.

Table (1): Velocity model used for locating and generating the Green's functions of kalabsha earthquakes (Simpson et al. 1986).

Depth (km)	Vp (km/s)	Vs (km/s)	Density (g/cm^3)
0.0	4.00	2.247	2.500
0.5	6.00	3.371	2.900
5.5	6.80	3.820	3.060
20.5	8.00	4.494	3.300

Table (2): Fault plane solutions and moment tensor elements of Kalabsha events, obtained from waveform inversion, the two fault planes are marked by (1) and (2).

Earthquake	Strike^0	Dip^0	Rake^0	Dc %	CLVD %
First event	(1) 26 (2) 44	37 59	-59 -111	84.6	15.4
Mrr	Mtt	Mpp	Mrt	Mrp	Mtp
-4.995	4.110	0.886	0.816	-2.754	2.196
Second event	(1) 233 (2) 39	40 50	-79 -99	74.7	24.3
Mrr	Mtt	Mpp	Mrt	Mrp	Mtp
-5.049	2.6112	2.437	-0.114	-1.103	1.950

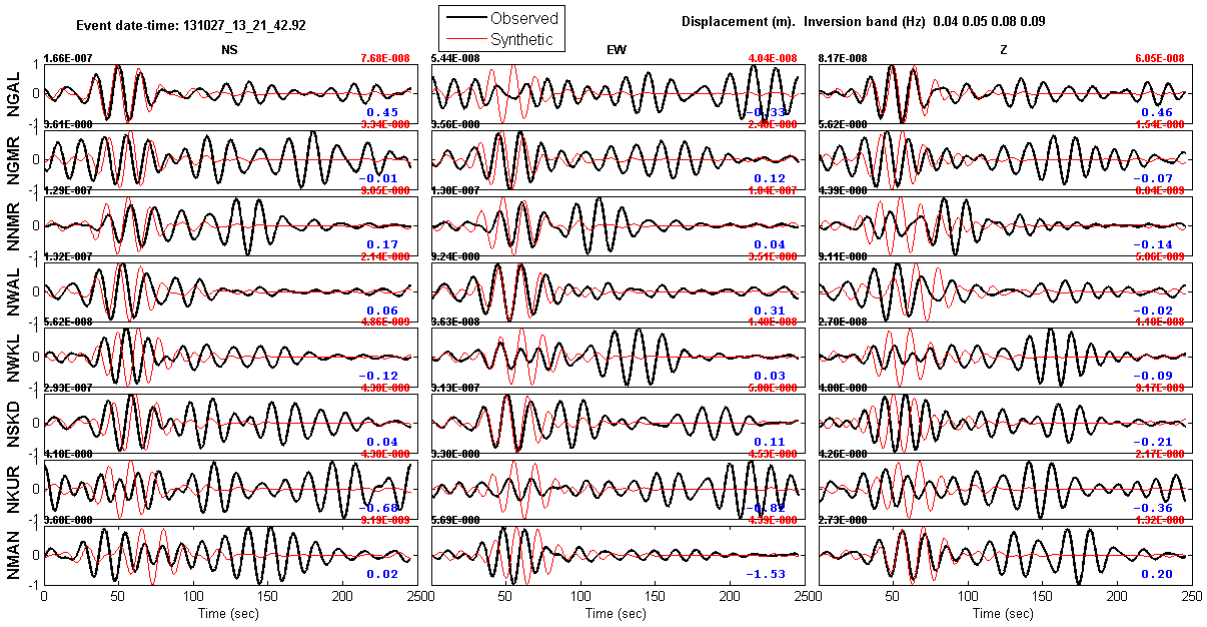

Fig. (4): Correlation between the observed and synthetic waveform seismograms used in the inversion. Name of each seismic station used in the inversion is marked beside each station. The three waveform components (NS, EW, and Z) are represented by three columns from left to right, respectively, for first event.

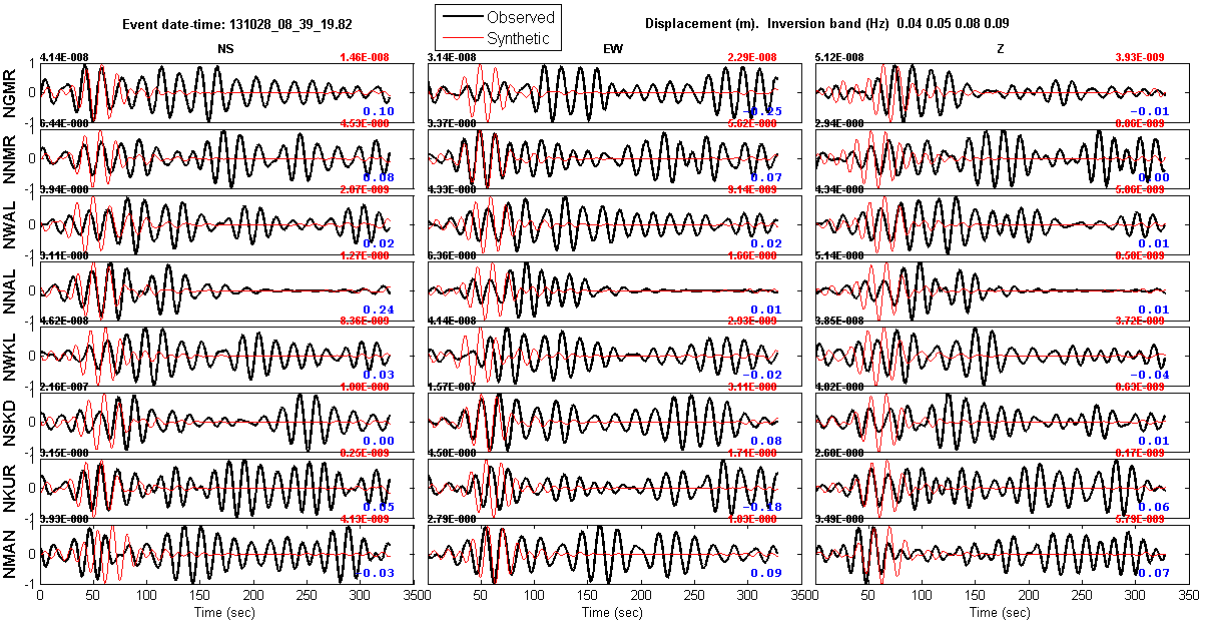

Fig. (5): Correlation between the observed and synthetic waveform seismograms used in the inversion. Name of each seismic station used in the inversion is marked beside each station. The three waveform components (NS, EW, and Z) are represented by three columns from left to right, respectively, for second event.

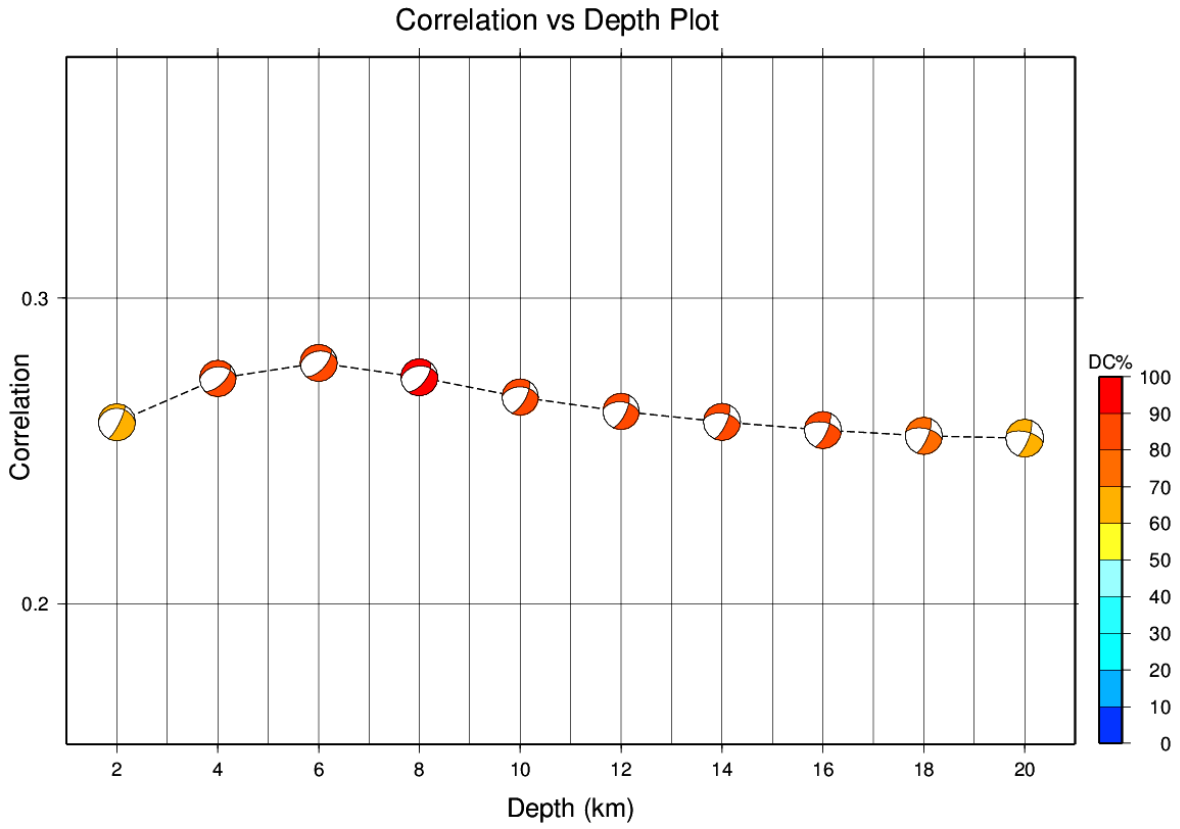

Fig. (6): The correlation of focal mechanism as a function of the trial source depth below the epicenter of ENSN (horizontal source position) for first event.

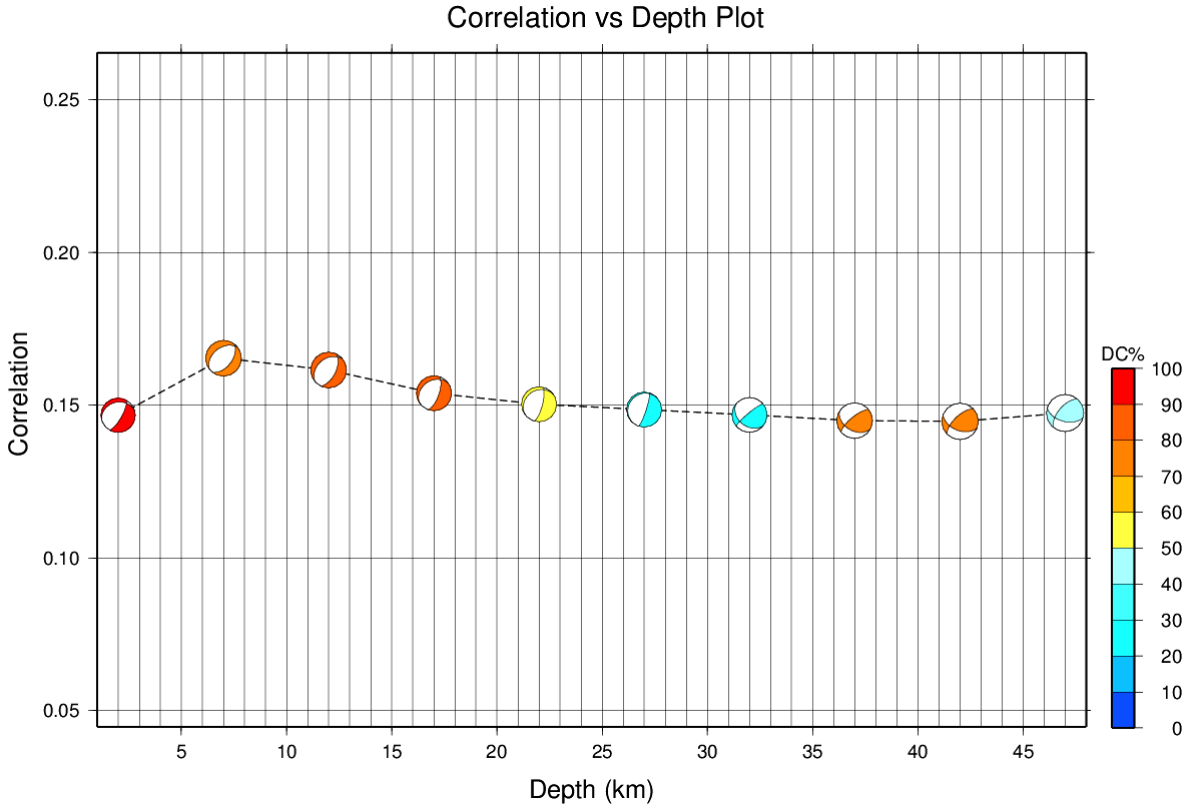

Fig. (7): The correlation of focal mechanism as a function of the trial source depth below the epicenter of ENSN (horizontal source position) for second event.

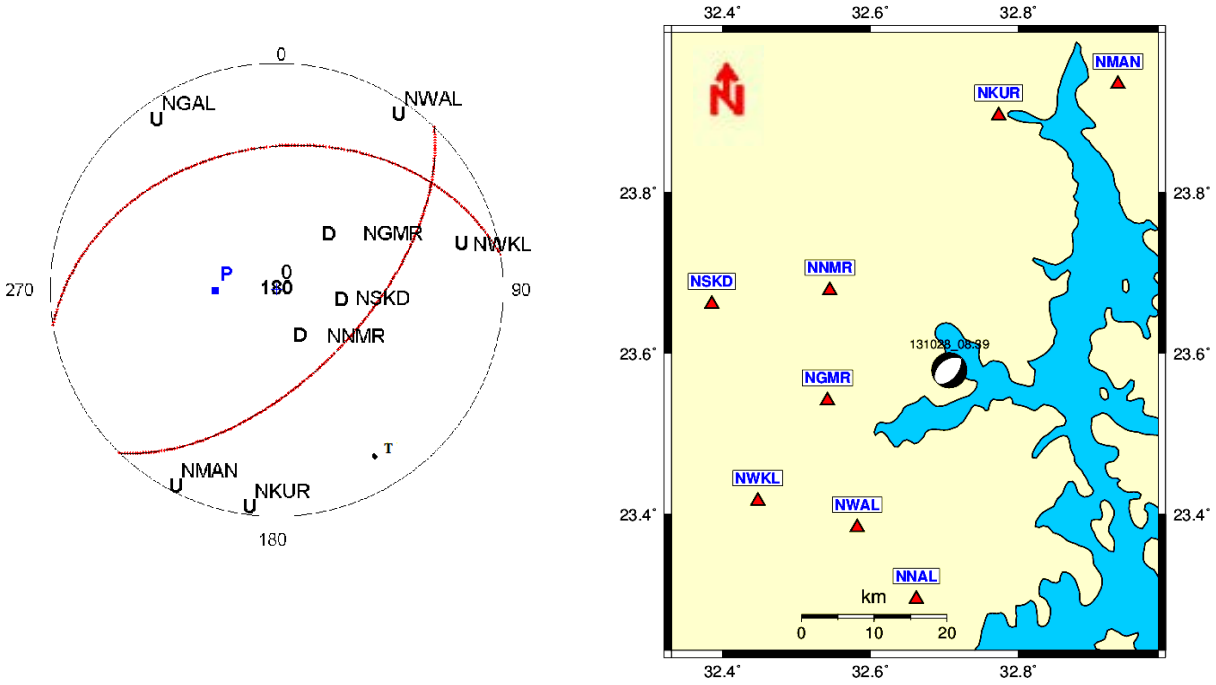

Fig. (8): Fault plane solutions of the Kalabsha earthquake indicate Strike slip with minor normal fault. (NGAL, NGMR, NNMR, NKWL, NWAL, NMAN , NKUR and NSKD) are used in the inversion for first event.

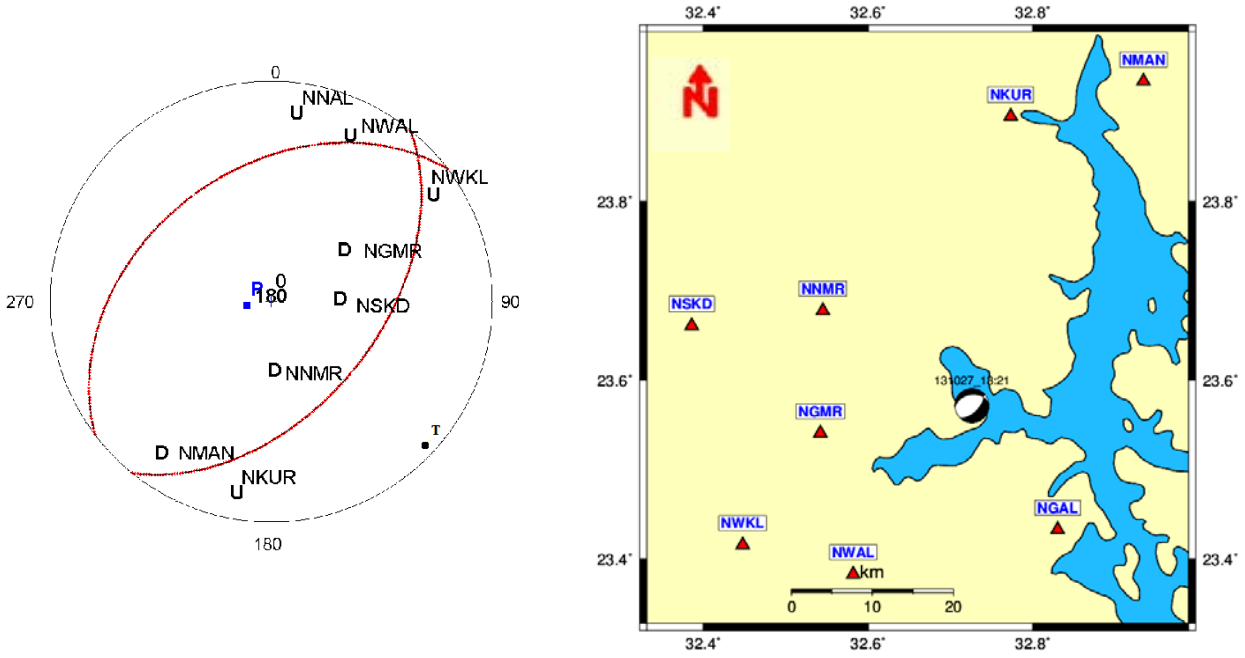

Fig. (9): Fault plane solutions of the Kalabsha earthquake indicate Strike slip with minor normal fault. (NNAl, NGMR, NNMR, NKWL, NWAL, NMAN, NKUR and NSKD are used in the inversion for second event.

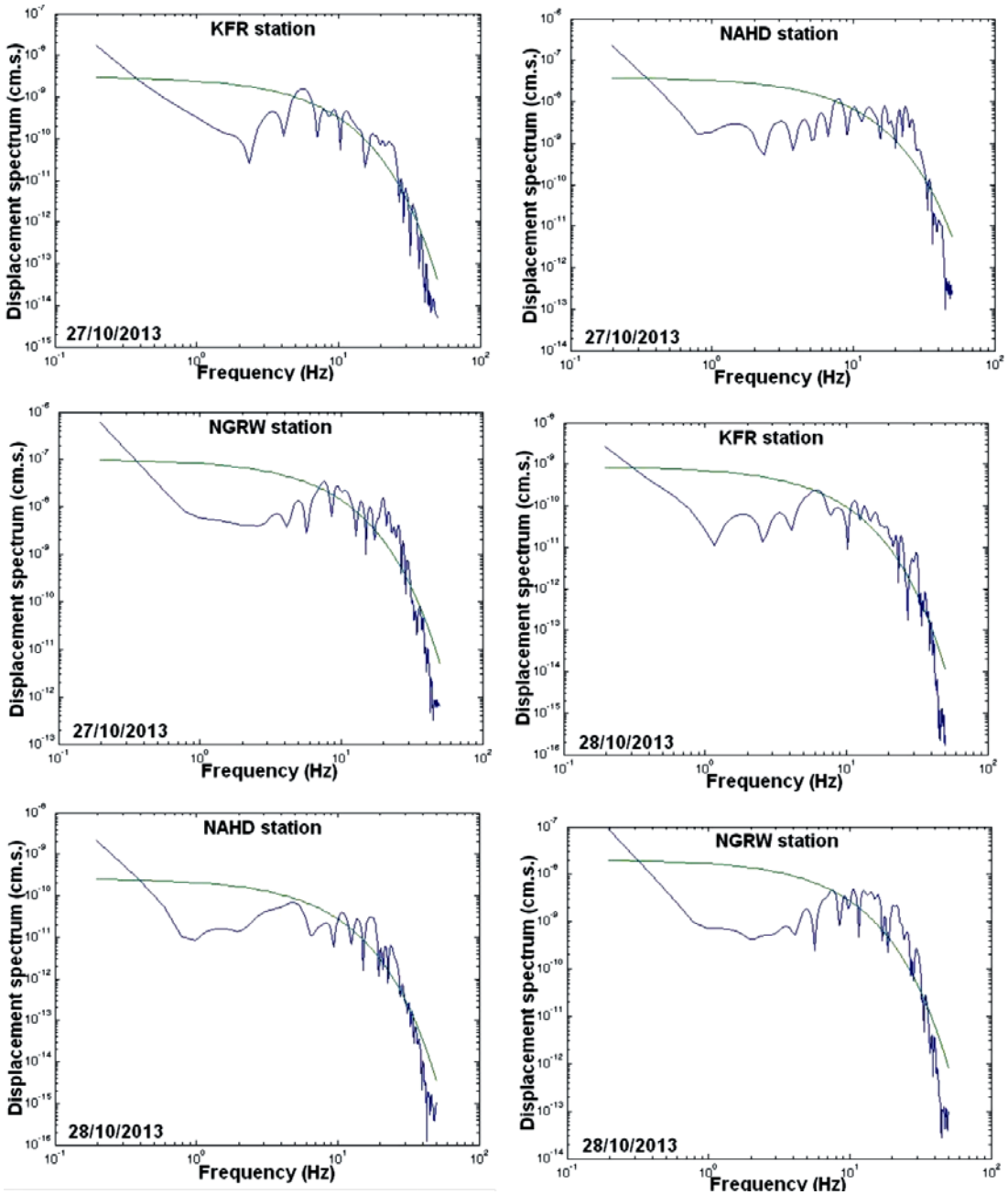

Fig. (10): Examples of earthquake spectra for some ENSN stations for the first event (first three figures) and the second event (other three figures).

Table (3): Estimated source parameters and of first event.

Lat. N^0	Lon. E^0	Depth Km	Mag. ML	Ω_0 cm-sec	f_c Hz	M_0 dyne.cm	r m	$\Delta\sigma$ MPa	Mag. MW	E erg
23.57	32.72	3.5	3.9	8.29E-09 ±2.067	24.36 ±0.1	6.18E+20 ±2.07	98.73 ±0.1	0.003 ±2.1	3.1 ±0.2	3.09E+16 ±2.07

Table (4): Estimated source parameters of second event

Lat. N⁰	**Lon. E⁰**	**Depth Km**	**Mag. ML**	**Ω 0 cm-sec**	**f_c Hz**	**M_0 dyne.cm**	***r* m**	**Δσ MPa**	**Mag. MW**	**E erg**
23.58	32.70	12.51	2.7	2.21E-09 ±1.68	24.10 ±0.1	1.95E+19 ±1.59	99.79 ±0.1	0.0008 ±1.5	2.1 ±0.2	9.74E+14 ±1.59

The obtained double-couple component is 84.6 % and the non-double component is 15.4% for the first event and the obtained double-couple component is 74.7 % and the non-double component is 25.3 % for second event. This non-double component could be due to artifacts of the velocity model used in the inversion or limited azimuth coverage, and the obtained fault plane solutions of the Kalabsha events, as listed in table (2).

4. SOURCE PARAMETERS

To calculate the source parameters of the first event and the second event the records of vertical component to every station were corrected to zero baseline and instrument response. We selected 2s P-wave signal windows that avoid contamination from other phases and maintain the resolution and stability of the spectra (Fig. 10).

The average spectrum was inverted using the simplified functional form of the source spectrum with a single corner frequency, described by the Boatwright (1978, 1980) equation:

$$S(f) = \Omega_0 / [1 + (f / f_c)^{2\gamma}]^{1/2} \quad (1)$$

In equation (1), the spectral parameters Ω_o, *f*c, and γ represent the low-frequency amplitude level, the corner frequency, and the high-frequency spectral fall-off beyond the corner frequency, respectively. By assuming Brume's model ($\gamma = 2$).

Source parameters (seismic moment, stress drop, and source radius) were then calculated for two events (Tables 3&4). The seismic moment (M_0) was estimated by the

following relationship (e.g., Brune 1970):

$$M_0 = 4\pi\rho v^3 R \Omega_0 / R_{(\theta,\varphi)} \quad (2)$$

Where ρ is the density of the medium (2700 kg/m^3), *R* is the hypocentral distance, *v* is the wave velocity, Ω_0 is the low frequency spectral amplitude and $R_{(\theta,\varphi)}$ is the radiation pattern coefficient. The estimated seismic moments (M_0) are 6.18E+20 dyne.cm for the first event and 1.95E+19 dyne.cm for the second event, (Table3&4).

The source radius (*r*) and the stress drop (**Δσ**) were calculated following Madariaga (1976):

$$r = 0.37\, v / f_c \quad (3)$$

where *v* is the wave velocity, f_c is the corner frequency of the wave.

$$\Delta\sigma = 7/16\ (M_0 / r^3) \quad (4)$$

where M_o is the seismic moment and *r* is the fault radius.

5. ENERGY RELEASED

For the average earthquakes, the seismic wave energy (E) is related by the equation (5), (Kanamori, 1977). Seismic energy released (E) is calculated for the two earthquakes by equation (5) as shown in table (3&4).

$$E = Mo / (2 \times 10^4)\ \text{erg}\ (1\ \text{erg} = 1\ \text{dyne cm}) \quad (5)$$

6. DISCUSSION AND CONCLUSIONS

Generally, The present day tectonic deformations within Egypt are related to the regional tectonic forces of the surrounding plate boundaries including the African-Eurasian plate margin, the Red Sea plate margin, and the Levant transform fault in addition to the local tectonics in Egypt. Very important information about the tectonics of Egypt can be obtained from the spatial distribution of earthquakes and their derived mechanisms. In the southern part of Egypt, based on the background seismicity (14 November 1981 event, earthquake swarms, 2004, in addition to some moderate earthquakes), the Aswan area is considered a locally active seismic area.

On October 27, 2013 at 13:21:15 (GMT) an earthquake of ML 3.9 occurred west Lake Nasser and followed with earthquake on October 28, 2013 at 08:39:19 (GMT) an earthquake of ML 2.7 on the Kalabsha fault at the Aswan area on the west bank of Lake Nasser. These earthquakes occurred on the Kalabsha fault at the eastern part of the fault with a depth of 3.5 and 12.15 km, respectively, and towards the west bank of Lake Nasser,(Tables 3&4).,

The obtained source mechanism indicates strike slip with normal faulting movement trending to NE–SW, which agrees with the trend of faults within Kalabsha area. The best fitting depth was 6 and 7 km. The earthquakes were mostly double-couple 84.6 and 74.7, but had 15.4 and 25.3 % non-double-couple component (CLVD) compensated linear-vector dipole.

Source parameters, such as seismic moment (Mo), fault radius (r), corner frequency (fc), and the stress drop (Δσ) were calculated for those events. Seismic

moment is measured at 6.18E+20 and 1.95E+19 dyne.cm, the fault radius at 98.73 and 99.79 m, the average corner frequency, fc is about 24.63 and 24.10 Hz, and the stress drop is 0.003 and 0.0008 MPa.

We use seismic moment values to estimate moment magnitudes, the small stress drop and big fault radius due to the tectonic situation closer to plate boundaries.

When considering the occurrence of these events and other background seismicity, we conclude that the seismic activity of the Aswan area is related to the local, regional, and global stresses. The regional stress is generated by the Red Sea rift system; the local one could be coming from the load pore pressure of Lake Nasser reservoir. And this serves as triggering the release of preexisting stress stored in the earth's crust. The global stresses could be due to the African-Eurasian margin plate. Then, we conclude that the Aswan area, which has been considered as an active seismic area, is still active.

Acknowledgments:

The authors would like to express their gratitude and appreciation to their colleagues at the Seismology Department, Egyptian National Seismological Network ENSN who analyzed the waveform of the Kalabsha earthquakes, used in the present study.

REFERENCES

Abou Elenean, K. M. (2007). Focal mechanisms of small and moderate size earthquakes recorded by the Egyptian National Seismic Network (ENSN), Egypt. NRIAG J Geophys 6:119–153.

Awad, H. (1994). Investigation of the tectonic setting, seismic activity and crustal deformation in Aswan seismic region, Egypt, Ph.D. Thesis,Tokyo University (unpublished).

Awad, H. and Mizoue, M. (1995). Earthquake activity in the Aswan region.Egypt Pageoph 145:69–86

Awad, H. (2002). Seismicity and water level variations in the Lake Aswan area in Egypt 1982–1997. J Seismol 6:459.

Boatwright, J. (1978). Detailed spectral analysis of Two small New York state earthquakes. Bull. Seismol. Soc. Am. Vol. 69, p. 49-79.

Boatwright, J. (1980). A spectral theory for circular seismic sources: simple estimates of source dimension, dynamic stress drop and radiated energy, Bull. Seism. Soc. Am. 70, 1–27.

Bouchon, M. (2003). A review of the discrete wave number method. Pure Appl. Geophys 160(3–4): 445–465.

Brune, J. N. (1970). Tectonic stress and spectra of seismi~ shear waves from earthquakes, J. Geophys. Res., 75, 4997-5009.

Campus, P. and Faeh, D. (1997). Seismic monitoring of explosions: a method to extract information on the isotropic component of the seismic source, J. Seismol. 1, 205–218.

Coutant, O. (1990). Program of numerical simulation AXITRA,Laboratoire de Geophysique Interne et Tectonophysique Report.University of Joseph Fourier (in French).

Dreger, D., and B.Woods (2002). Regional distance seismic moment tensors of nuclear explosions, Tectonophysics 356, 139–156.

El-Hady, S. M., Khalil, A. E., and Hosny, A. (2004). 1-D velocity structure in Northern of Aswan Lake, Egypt deduced from travel time data. J Appl Geophys 3(1):55–62.

Elshazly, E. M. (1977). The geology of the Egyptian region. Ocean Basin Margins 145:193–207.

Fat-Helbary, R. and Tealeb, A. (2000). A study of seismicity and earthquake loading at the proposed Kalabsha Dam site, Aswan, Egypt. Bulletin of NRIAG, vol B, pp 39-61.

Frohlich, C. (1994). Earthquakes with non-double-couple mechanisms, Science 264, 804-809.

Hassib, G. H. (1990). A study on the earthquake mechanics around the high dam lake, Aswan, Egypt, Ph.D. Thesis, Faculty of Science. South Valley University, Sohag.

Hassib, G. H. (1997). A study on the earthquake mechanics around the High Dam Lake, Aswan, Egypt. Ph.D. Thesis, Faculty of Science. South Valley University, Sohag.

Issawi, B. (1978). Geology of Nubia, West area, Western Desert, Egypt.Annals Geol Surv Egypt 3:327–392.

Issawi, B. (1982). Geology of the southwestern desert of Egypt, Ann Geol Survey Egypt.

Woodward-Clyde Consultants (1985) Earthquake activity and stability evaluation for Aswan High Dam; Unpublished report, High and Aswan Dam Authority. Ministry of Irrigation, Egypt.

Kanamori, H. (1977). The energy release in great earthquakes. JGeophys Res 82:2981–2987.

Ahmed Hosny & Sherif M. Ali & Azza Abed (2013). Study of the 26 December 2011 Aswan earthquake,Aswan area, South of Egypt, Arab J Geosci.

Kebeasy, R. M., Maamon, M., and Ibrahim, E. M. (1982). Aswan Lake induced earthquake. Bull Intern Inst Seismol Earth Eng Tsukuba 19:155–160.

Kebeasy, R. M., Maamoun, MM., Ibrahim, E. M., Megahed, A., Simpson, D.W. and Leith, W.L. (1987). Earthquake studies at Aswan Reservoir. J Geodyn 7:173–193.

Kebeasy, R. M. and Gharib, A. A. (1991). Active fault and water loading are important factors in triggering earthquake activity around Aswan Lake. J Geodyn 14:73–82.

Kebeasy, R. M. and Tealeb A. A. (1997). Earthquake activity and subsurface structures of south valley project., internal report, NRIAG, 14: 27p.

Khalil, A. E., El-Hady, S. M. and Hosny, A. (2004). Three-dimensional velocity structure of VP and VP/VS around Aswan area, Egypt. J Appl Geophys 3(1):303–314.

Kikuchi, M. and Kanamori, H. (1991). Inversion of complex body waves-III.Bull Seis Soc Am 81:2335-2350.

Madariaga, R. (1976). Dynamics of an expanding circular fault. Bull Seism. Soc. Am. 66, 639-666.

Mahmoud, S. M. (1994). Geodetic and seismotectonic deformation near Aswan reservoir, Egypt. Bulletin of CRCM No.41. Praha, Czech Republic. pp 5-30.

Mekkawi, M., Grasso, J-R. and Schnegg, P-A. (2004). A long-lasting relaxation of seismicity at Aswan, Egypt, 1982–2001. Bull Seism Soc Am 94:479–492.

Mekkawi, M. Abdel-Monem, S.M., Rayan, A. Mahmoud, S., Saleh, A. and Moustafa, S. (2008). Subsurface Tectonic Structure and Crustal Deformation at Kalabsh fault, Aswan, Egypt fromMagnetic, GPS, and Seismic data, NRIAG, J Geophys, special issue, pp 681–700.

Simpson, D.W., Gharib, A., and Kebeasy, R. M., (1986). Induced Seismicity and changes in water level at Aswan reservoir, Egypt: Gerlands Beitr. Geophysik. Leipzig, vol. 99 (3), pp. 191-204.

Simpson, D.W., Gharib, A. A. and Kebeasy, R.M. (1990). Induced seismicity and changes in water level at Aswan reservoir, Egypt. Gerlands Beitr Geophys Leipzig 99:191–204.

Sokos, E. and Zahradnı'k, J. (2008). ISOLA: a Fortran code and a Matlab GUI to perform multiple-point source inversion of seismic data.Comput Geosci doi:10.1016/j.cageo. 2007.07.005.

Taha, Y. S. (1997). Evaluation of the crustal structure setting of Aswan area, Ph.D. thesis, Faculty of Science, Cairo University, Egypt, 152 p.

Tealeb, A. (1999). proposed programs for monitoring crustal deformations at seismo active area of Aswan, Egypt using geodetic techniques.Internal Report at NRIAG, 81p.

Thorne, M. S. (2005). Broadband waveform modelling of deep mantle structure. Ph.D, Dissertation Thesis, Arizona State University,Arizona.

Woodward-Clyde Consultants (1985). Earthquake activity and stability evaluation for Aswan High Dam; Unpublished report, High and Aswan Dam Authority. Ministry of Irrigation, Egypt.

Zahradnik, J. and Plesinger, A. (2005). Long-period pulses in broadband records of near earthquakes. Bull Seismol Soc Am 95:1928–1939.